

# Ultrafast optical delay line by use of a time-prism pair

James van Howe and Chris Xu

School of Applied and Engineering Physics, Cornell University, Ithaca, New York 14853

Received July 26, 2004

We demonstrate an all-fiber, programmable, ultrafast optical delay line based on reversible frequency conversion by use of a time-prism pair. Using electro-optic phase modulators to provide the time-prism phase profile, we show a record scanning rate of 0.5 GHz and a delay range of 19.0 ps. Computer modeling suggests that aberration correction in the time-prism system can extend the delay range to 28.0 ps. Finally, limitations and potential improvement of our techniques are discussed. © 2005 Optical Society of America

OCIS codes: 320.7160, 070.2580, 070.6020.

Optical delay lines with programmable delays, fine resolution, and rapid scanning are necessary for a variety of applications, such as optical coherence tomography, optical metrology, interferometry, and telecommunications.<sup>1,2</sup> Techniques with the fastest scanning include the use of acousto-optic modulators or deflectors to achieve scanning rates of the order of 1 MHz.<sup>1,2</sup> Other techniques make use of grating-based dispersive optics and scanning mirrors to obtain scanning rates of the order of 1 kHz.<sup>3–6</sup> Using a time-prism pair, we demonstrate an all-fiber, programmable, ultrafast optical delay line with a record scanning rate of 0.5 GHz and a range of 19 ps. Furthermore, we show through computer modeling that applying an aberration correction technique to eliminate nonlinearities in the phase profile of each time prism can significantly improve the performance of our system.

A time prism works by converting the frequency of an incoming electric field. Any amount of dispersion following the prism results in a displacement of the electric field in time. Another time prism can be used to convert the frequency back to its original value, with the resultant field being the original electric field but delayed in time. This is analogous to a spatial prism pair, which changes the  $\mathbf{k}$  vector of the incoming field, resulting in a displacement in space. The second prism converts the  $\mathbf{k}$  vector back to its original value, with the resultant field being the original electric field translated in space. Mathematically, a time prism imposes a linear phase in time onto an incoming electric field just as a spatial prism does in space. Our method utilizes a sinusoidally driven LiNbO<sub>3</sub> phase modulator to achieve this phase profile:

$$\varphi = \pi \frac{V}{2V_\pi} \sin(2\pi f_m t) \approx \pi^2 \frac{V}{V_\pi} f_m t. \quad (1)$$

Here the sine term has been expanded to first order,  $f_m$  is the modulation frequency,  $V$  is the peak-to-peak drive voltage, and  $V_\pi$  is the voltage required to obtain a  $\pi$  phase shift. The frequency of the incoming optical field is therefore shifted by an amount  $\Delta\omega = d\varphi/dt = \pi^2(V/V_\pi)f_m$ . Using a fiber of dispersion value  $D$  (ps/nm) after a time prism introduces a delay

$$\Delta\tau = \Delta\lambda D = \pi \frac{\lambda^2}{2c} \frac{V}{V_\pi} f_m D, \quad (2)$$

where  $\lambda$  is the center wavelength of the incident pulse train and  $\Delta\lambda = (\lambda^2/2\pi c)\Delta\omega$  is the corresponding wavelength shift that is due to phase modulation. Tuning the drive voltage of the time prism is analogous to changing the apex angle of a spatial prism. In either case one changes the phase slope, thereby changing the frequency ( $\mathbf{k}$  vector) and hence the delay (spatial translation). To convert the frequency of the optical field back to its original value, one need only impose a phase  $-\Delta\omega t$ , which can be easily accomplished by another LiNbO<sub>3</sub> phase modulator driven with the same sinusoid but  $\pi$  out of phase. Such an approach to frequency conversion with electro-optic phase modulation has been used in the past for other applications.<sup>7–9</sup>

The experimental setup is shown in Fig. 1. The pulsed source consisted of an 8-ps pulse train at a

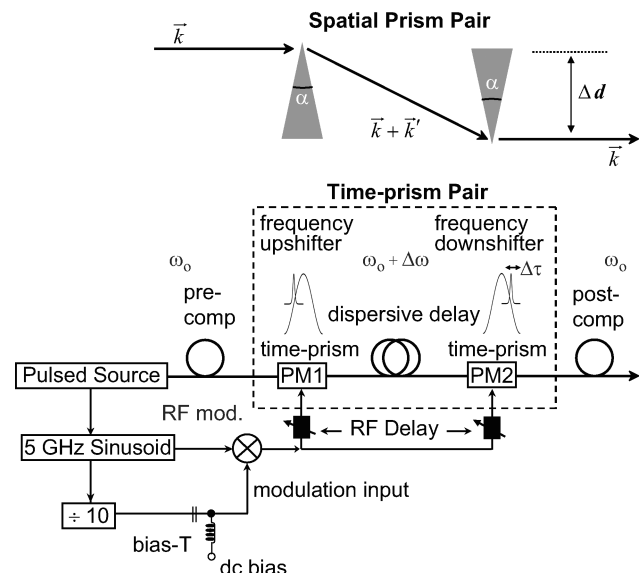


Fig. 1. Experimental setup. The pulsed source emits an 8.0-ps, 5-GHz pulse train generated by pulse carving and time-lens compression.<sup>10</sup> The pulse train is precompensated and postcompensated (pre-comp and post-comp) by fiber spools with a dispersion value of 37.0 ps/nm each. The time prisms (phase modulators PM1 and PM2) are each driven by a 5-GHz sinusoid whose amplitude is modulated by the modulation input to the rf modulator. A dispersive delay of  $-74.0$  ps/nm is used for generating the time delay. A schematic of a spatial prism pair is shown above to demonstrate the space-time analogy.

5-GHz repetition rate, generated by pulse-carving cw light and time-lens compression.<sup>10</sup> Pulses were upshifted in frequency by the first time prism, a sinusoidally driven LiNbO<sub>3</sub> phase modulator (PM1). A time delay was then introduced by the dispersive delay, which consisted of 0.7 km of dispersion-compensating fiber (total dispersion value of  $D = -74$  ps/nm). The second time prism, a phase modulator driven with the same sinusoid but  $\pi$  out of phase (PM2), was used to downshift the frequencies back to their original values. Dispersion precompensation (37 ps/nm) and postcompensation (37 ps/nm) were used to eliminate the pulse-broadening effects caused by the dispersive delay and to achieve symmetrical operations for the frequency shifters, thus ensuring pulse delay without the adverse effect of pulse distortion. To vary the frequency shift and therefore the delay, the drive voltage to the phase modulators was adjusted through a broadband rf modulator (Minicircuits, ZMX-7GMH). The rf modulator controls the drive voltage to the optical phase modulators so that the resulting time delay from Eq. (2) is

$$\Delta\tau = \Delta\lambda D \propto V \propto V_{\text{rf\_mod}}, \quad (3)$$

where  $V_{\text{rf\_mod}}$  is the modulation input into the rf modulator. Thus ultrafast programmable time delays can be obtained by controlling the modulation waveform  $V_{\text{rf\_mod}}$ .

To demonstrate the concept, we first modulated the 5-GHz rf input with dc voltages through the bias T. Figures 2(a) and 2(b) show the dependence of the frequency shift and corresponding time delay on modulation input  $V_{\text{rf\_mod}}$ . A frequency shift of 32.5 GHz is achieved at the highest rf output into the phase modulator ( $V \sim 4.24V_{\pi}$ ), which results in a time delay of 19 ps. These results agree well with Eq. (2). The nonzero intercept of the data in Fig. 2 is characteristic of the rf modulator, which uses diodes as time-varying switches. The diode drop required for biasing these switches on is responsible for the offset in intercept. We demonstrate the ultrafast scanning capability of our delay line by modulating the rf input with a sinusoidal waveform at 0.5 GHz. Figure 3(a) shows the oscilloscope trace of a portion of the pulse train. The corresponding delays are plotted in Fig. 3(b), showing the precise mapping of modulation input  $V_{\text{rf\_mod}}$  to the time delay. Figure 4(a) shows the original spectrum, and Fig. 4(b) shows the calculated and measured spectra after frequency upshifting (PM1). The excellent match between measurement and theory demonstrates the system's robustness and predictability.

Care was taken in choosing parameters in the setup to ensure that as much energy as possible of the optical pulses was placed over the linear portion of the electrical sinusoidal drive both for frequency upshifting and downshifting while simultaneously maximizing the amount of time delay. This is important because higher-order terms in the phase modulation drive are responsible for distortions in both the spectral and the temporal pulse profiles. Any nonlinear modulation terms in the frequency upshift drive will chirp the

pulses and lead to compression or broadening if they are not unchirped by frequency downshifting. This unchirping is difficult to apply to every pulse, each of which will have a different time delay and will therefore be frequency downshifted by a different portion of the downshifting sinusoid, some of which are more nonlinear than others. This results in the inability to convert the spectrum of the upshifted optical field back to the original, and therefore results in variation in pulse intensity, width, and shape. Our system exhibited small distortions that are due to this nonlinearity that is seen in the 1.0% variation in optical intensity of delayed pulses in Fig. 3(a). Failure to completely restore the original optical spectrum can be seen in Fig. 5(a), which shows the spectrum after frequency downshifting (after PM2) for the worst-case scenario (the case of highest frequency upshift, 32.5 GHz, corresponding to the highest dc modulation input into the bias T). This incomplete spectral match agrees well with our simulations.

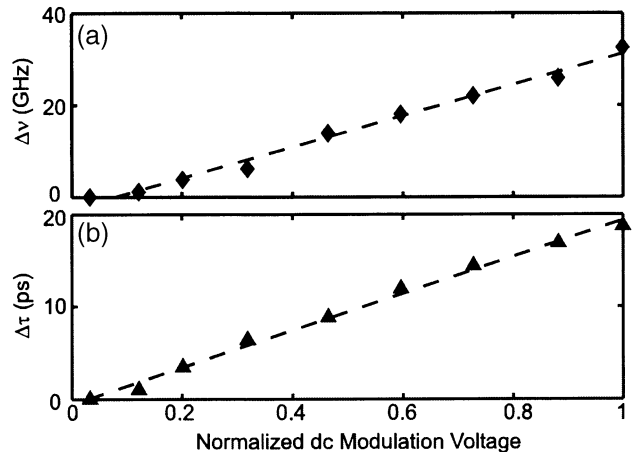


Fig. 2. (a) Frequency shift ( $\Delta\nu$ ) versus the applied dc modulation input. (b) Corresponding time delay ( $\Delta\tau$ ) at each frequency shift. Dashed lines were drawn to aid the eye.

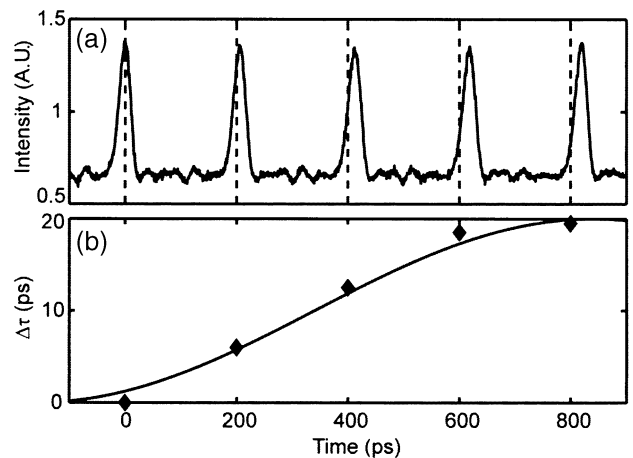


Fig. 3. (a) Oscilloscope time trace demonstrating the rapid scanning of the time delays. The dashed grid lines indicate the original pulse positions with no phase modulation. (b) Delay ( $\Delta\tau$ ) as a function of time obtained from (a). The solid curve shows the 0.5-GHz sinusoidal envelope function of the drive voltage into the phase modulators.

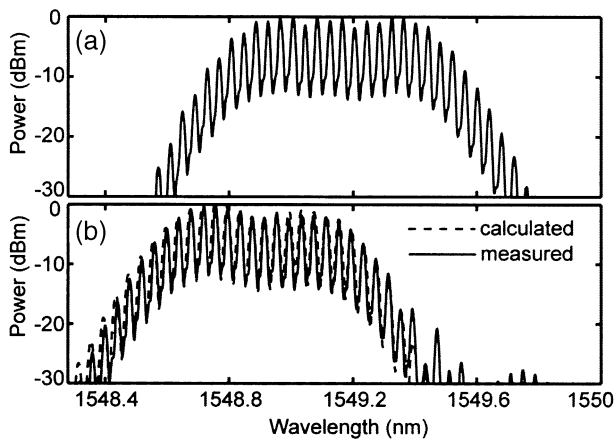


Fig. 4. Optical spectra (a) of the original pulse train and (b) after frequency upshifting from the first time prism (PM1). The solid curve shows the measured spectrum, and the dashed curve shows the calculated spectrum. Resolution bandwidth on all the spectra is 0.01 nm.

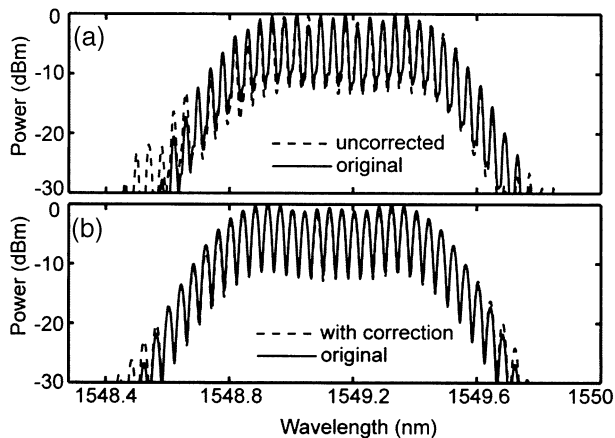


Fig. 5. (a) Optical spectra of delayed pulses after frequency downshifting from the second time prism (PM2) without correction (dashed curve) and the original spectrum (solid curve). (b) Calculated spectra in the case of aberration correction. The dashed curve shows the downshifted spectrum with the additional 15-GHz correction sinusoid. The solid curve shows the original spectrum. The resolution bandwidth of all the spectra is 0.01 nm.

The limitation of the nonlinear phase profile can be largely overcome by use of an improved drive waveform into the phase modulators. We show through computer modeling that adding a correction time prism, analogous to aberration correction in a time-lens system,<sup>10</sup> can reduce nonlinearity in the phase modulation drive and significantly reduce pulse distortion. Fourier analysis allows any periodic function to be decomposed into a sum of harmonics. In the case of an ideal triangle waveform the next-order term in the Fourier expansion is the third harmonic. Our calculations show that maximum reduction of the pulse distortion can be achieved by adding a sinusoidal drive at 15 GHz and a peak-to-peak amplitude

of  $0.29V_{\pi}$  (three times the frequency of the original time prism and 6.9% of the drive). The better match between the calculated original and reshifted spectra shown in Fig. 5(b) demonstrates the effectiveness of this correction technique. On the other hand, for spectral distortion comparable with that of the uncorrected system [Fig. 5(a)] the additional correction time prism increases the total delay to 28 ps. In terms of an initial pulse width of  $T_o = 8.0$  ps the correction prism extends the delay range from  $2.4T_o$  to  $3.5T_o$ . We note that, instead of a separate correction time-prism stage, it is possible to implement this correction technique by combining both the 5- and the 15-GHz drives into a single rf drive and therefore use a single phase modulator to obtain the same results.

In summary, we have demonstrated an all-fiber ultrafast optical delay line based on reversible frequency conversion by use of a time-prism pair. We show a record scanning rate of 0.5 GHz over a delay range of 19.0 ps. Computer modeling suggests that a 28.0-ps delay range can be obtained for the same system through the implementation of aberration correction by use of a correction time prism. Future improvements to the system could include replacing the fiber spools with other dispersive devices such as fiber Bragg gratings, making the system more compact, and eliminating the potential problems of slow timing wander owing to temperature fluctuations and long fiber lengths. Finally, scanning is not limited to the 0.5-GHz sinusoidal drive presented in this work but could consist of any desired rf waveform. Thus the demonstrated ultrafast delay line permits electronically controlled pulse position, delay range, and scan rate.

The authors gratefully acknowledge the loan of dispersion-compensating fiber by Dan Kilper of Lucent Technologies. J. van Howe's e-mail address is jwv9@cornell.edu.

## References

1. W. Yang, D. Keusters, D. Goswami, and W. S. Warren, *Opt. Lett.* **23**, 1843 (1998).
2. R. Piyaket, S. Hunter, J. E. Ford, and S. Esener, *Appl. Opt.* **34**, 1445 (1995).
3. A. M. Rollins, M. D. Kulkarni, S. Yazdanfar, R. Ung-arunyawee, and J. A. Izatt, *Opt. Express* **3**, 219 (1998), <http://www.opticsexpress.org>.
4. G. J. Tearney, B. E. Bouma, and J. G. Fujimoto, *Opt. Lett.* **22**, 1811 (1997).
5. X. Liu, M. J. Cobb, and X. Li, *Opt. Lett.* **29**, 80 (2004).
6. A. L. Oldenburg, J. J. Reynolds, D. L. Marks, and S. A. Boppart, *Appl. Opt.* **42**, 4606 (2003).
7. L. A. Jiang, M. E. Grein, H. A. Haus, and E. P. Ippen, *Opt. Lett.* **28**, 78 (2003).
8. I. Y. Poberezhskiy, B. J. Bortnik, S. Kim, and H. R. Fetterman, *Opt. Lett.* **28**, 1570 (2003).
9. L. F. Mollenauer and C. Xu, presented at the Conference on Lasers and Electro-Optics, Long Beach, Calif., May 19–24, 2002.
10. J. van Howe, J. Hansryd, and C. Xu, *Opt. Lett.* **29**, 1470 (2004).